Preferential Zn²⁺ influx through Ca²⁺-permeable AMPA/kainate channels triggers prolonged mitochondrial superoxide production

STEFANO L. SENSI*, HONG Z. YIN*, SEAN G. CARRIEDO†, SHYAM S. RAO‡, AND JOHN H. WEISS*‡†§

Departments of *Neurology, ‡Anatomy and Neurobiology, and †Psychobiology, University of California, Irvine, CA 92697-4292

ABSTRACT Synaptically released Zn²⁺ can enter and cause injury to postsynaptic neurons. Microfluorimetric studies using the Zn²⁺-sensitive probe, Newport green, examined levels of $[Zn^{2+}]_i$ attained in cultured cortical neurons on exposure to N-methyl-D-asparte, kainate, or high K⁺ (to activate voltage-sensitive Ca²⁺ channels) in the presence of 300 μM Zn²⁺. Indicating particularly high permeability through Ca²⁺-permeable α-amino3-hydroxy-5-methyl-4-isoxazolepropionic-acid/kainate (Ca-A/K) channels, micromolar $[Zn^{2+}]_i$ rises were observed only after kainate exposures and only in neurons expressing these channels [Ca-A/K(+) neurons]. Further studies using the oxidation-sensitive dye, hydroethidine, revealed Zn²⁺-dependent reactive oxygen species (ROS) generation that paralleled the $[Zn^{2+}]_i$ rises, with rapid oxidation observed only in the case of Zn²⁺ entry through Ca-A/K channels. Indicating a mitochondrial source of this ROS generation, hydroethidine oxidation was inhibited by the mitochondrial electron transport blocker, rotenone. Additional evidence for a direct interaction between Zn²⁺ and mitochondria was provided by the observation that the Zn²⁺ entry through Ca-A/K channels triggered rapid mitochondrial depolarization, as assessed by using the potential-sensitive dye tetramethylrhodamine ethylester. Whereas Ca²⁺ influx through Ca-A/K channels also triggers ROS production, the $[Zn^{2+}]_i$ rises and subsequent ROS production are of more prolonged duration.

In the brain, Zn²⁺ is sequestered at high concentrations in presynaptic boutons of many excitatory synapses (1, 2), and, when released with neuronal activity, is estimated to achieve peak synaptic concentrations of several hundred micromolar (3, 4). *In vivo*, seizure activity and ischemia have been associated with a depletion of presynaptic Zn²⁺ and concomitant Zn²⁺ accumulation in degenerating postsynaptic neurons (5–8). Blockade of this translocation by Zn²⁺ chelators was recently reported to decrease selective neurodegeneration in these conditions (8, 9). *In vitro*, neurotoxic effects of Zn²⁺ occur after entry through voltage-sensitive Ca²⁺ channels (VSCC; refs. 10–11), N-methyl-D-aspartate (NMDA) channels (12), or Ca²⁺-permeable α-amino3-hydroxy-5-methyl-4-isoxazolepropionic-acid (AMPA)/kainate channels (Ca-A/K channels; refs. 13, 14). Two lines of evidence led us to hypothesize that of these routes, Zn²⁺ permeates Ca-A/K channels most readily. First, neurotoxicity studies demonstrated that kainate exposures in the presence of low levels of Zn²⁺ triggered selective degeneration of neurons expressing these channels (13). In addition, by analogy to the kainate-activated Co²⁺ uptake stain that labels cells expressing Ca-A/K channels, kainate also triggers selective accumulation of histochemically detectable Zn²⁺ in these same neurons, while neither high-K⁺ nor NMDA triggered comparable uptake (14).

In a recent study, we pioneered the use of the relatively high-affinity Zn²⁺-sensitive fluorescent dye, mag-fura-5, to assess rapid agonist-stimulated rises in intracellular free Zn²⁺ ($\Delta[Zn^{2+}]_i$; ref. 15). However, we were concerned that the high affinity of mag-fura-5 for Zn²⁺ ($K_d \approx 27$ nM; ref. 15) might lead to underestimation of peak $\Delta[Zn^{2+}]_i$ values, much as has been observed in the case of agonist-stimulated $[Ca^{2+}]_i$ rises (16, 17). The present study had two primary aims. The first was to quantitatively compare $\Delta[Zn^{2+}]_i$ resulting after Zn²⁺ exposure during activation of NMDA channels, VSCC, or Ca-A/K channels, by using a lower-affinity fluorescent probe (Newport green; $K_d \approx 1$ μM; ref. 18). The second was to examine downstream effects of Zn²⁺ entry that might lead to neuronal injury. Specifically, rapid Ca²⁺ entry has been found to trigger generation of injurious reactive oxygen species (ROS) (17, 19–22). Thus, by analogy with this Ca²⁺ effect, we tested the hypothesis that rapid Zn²⁺ entry through Ca-A/K channels also triggers rapid ROS production, by using the oxidation-sensitive dye hydroethidine (HEt; ref. 22).

MATERIALS AND METHODS

Chemicals and Reagents. HEt, tetramethylrhodamine ethylester (TMRE), fura-2, and Newport green were purchased from Molecular Probes. Fura-2FF was purchased from TefLabs (Austin, TX). MK-801 was purchased from Research Biochemicals (Natick, MA). Tissue culture media and serum were from Life Technologies (Grand Island, NY). 2,3-dihydroxy-6-nitro-7-sulfamoyl-benzo(F)quinoxaline (NBQX) was kindly provided by Novo-Nordisk (Copenhagen) and U74500A from Upjohn (Kalamazoo, MI). NMDA, kainate, and rotenone were obtained from Sigma. All other chemicals and reagents were obtained from common commercial sources.

Cortical Cultures. Cultures were prepared largely as described previously (23). Briefly, dissociated mixed neocortical cell suspensions were prepared from 14- to 16-day-old embryonic Swiss–Webster mice and plated ($1–2 \times 10^5$ cells per cm²) on previously established astrocytic monolayers in either 24-well plates or glass-bottomed dishes (Plastek Cultureware, Ashland, MA). After 4–6 DIV (days *in vitro*), nonneuronal cell division was halted by exposure to 10^{-5} cytosine arabinoside for 24 h. The same procedure was used to prepare glial cultures, except that tissue was obtained from early postnatal (1–3 d) mice, media was supplemented with epidermal growth factor (10 ng/ml), and cell suspensions were plated directly on the plates or the polylysine- and laminin-coated coverslips.

Imaging Studies. Cultures were mounted on the stage of a Nikon Diaphot inverted microscope equipped with a 75 W xenon lamp, a computer-controlled filter wheel, and a 40×1.3 numerical aperture epifluorescence oil-immersion objective. Emitted signals were acquired with a Hamamatsu intensified charge-coupled device camera and digitized by using IMAGE 1/FLUOR software (Universal Imaging, West Chester, PA). Neutral density filters were used to minimize photobleaching. Background fluorescence was subtracted from images (16 frame averages) at the beginning of each experiment.

For $[Ca^{2+}]_i$ and $[Zn^{2+}]_i$ imaging, cultures were loaded in the dark, with 5 μM of either Newport green diacetate (for Zn^{2+}), or with the acetoxymethyl ester of fura-2 or Fura-2FF (for Ca^{2+}) in a Hepes-buffered medium [(HSS) whose composition was (in mM): 120 NaCl, 5.4 KCl, 0.8 $MgCl_2$, 20 Hepes, 15 glucose, 1.8 $CaCl_2$, 10 NaOH, pH 7.4], containing 0.2% pluronic acid and 1.5% dimethyl sulfoxide (DMSO) for 30 min at 25°C, then washed in HSS and kept in the dark for an additional 30 min. For Newport green, excitation was 490 nm and emission at 530 nm. For the ratiometric dyes, fura-2 and Fura-2FF, excitation was at 340 and 380 nm, with emission at 510 nm. Experiments were carried out at room temperature (25°C) under constant perfusion with HSS. Drugs were added to the buffer, as indicated.

$[Zn^{2+}]_i$ was calculated by the following equation: $[Zn^{2+}]_i = K_d$ $(F-F_{min}/F_{max}-F)$ (24), where K_d is 1 μM (18). F_{max} was obtained at the end of each experiment by adding the Zn^{2+}-selective ionophore Na^+-pyrithione (10 μM) in the presence of 1 mM Zn^{2+} (the fluorescence rapidly approached a maximum) and F_{min} obtained (after Zn^{2+} washout) by adding the cell-permeable Zn^{2+} chelator N, N,N′,N′-tetrakis (2-pyridylmethyl)ethylenediamine (50 μM; ref. 25). $[Ca^{2+}]_i$ was determined by the following equation: $[Ca^{2+}]_i = K_d \cdot \beta \cdot [(R-R_{min})/(R_{max}-R)]$, where $\beta = F_{380\ free}/F_{380\ bound}$. K_d was 35 μM for Fura-2FF (26) and 225 nM for fura-2 (24).

Oxygen radical production and changes in mitochondrial polarization ($\Delta\psi$) were monitored by using the oxidation-sensitive dye HEt and the $\Delta\psi$-sensitive dye TMRE (17, 27), respectively. Cultures were loaded in the dark with 5 μM HEt in HSS (45 min) or 0.05 μM TMRE (30 min), both at 25°C. After loading, cultures were washed (four times) into a static bath of Ca^{2+}-free HSS containing either probe. Cells were excited at 510–560 nm and emission monitored at >590 nm. Camera gain was adjusted to give baseline maximal fluorescence levels of 20–40 (HEt experiments) or of 150–200 (TMRE experiments) arbitrary units of a maximal eight-bit signal output of 256. Fluorescence measurements for each cell (F_x) were normalized to the fluorescence intensity for that cell at the beginning of the experiment (F_0). In the TMRE experiments, fluorescence changes were monitored only in "mitochondria-rich" perinuclear regions of the soma, which undergo sharp decreases in fluorescence on mitochondrial depolarization. In HEt experiments, ROS production causes an increase in somatic and nuclear fluorescence.

Neurotoxicity Experiments. Toxic exposures to kainate (50 μM + 10 μM MK-801) + Zn^{2+} (50 μM) were for 5 min in HSS (25°C). Exposures were terminated by replacing the exposure solution bicarbonate containing media with 10 μM MK-801/10 μM NBQX and returning the cultures to the incubator. Overall neuronal injury was assessed 20–24 hr later by morphological examination and by measurement of lactate dehydrogenase release (28) and Ca-A/K(+) neuronal injury assessed by direct cell counts of intact $Co^{2+}(+)$ neurons compared with numbers present in sister cultures exposed to sham wash alone.

Identification of Neurons Highly Expressing Ca-A/K Channels [Ca-A/K(+) Neurons]. Two techniques were used to identify Ca-A/K(+) neurons. In most cases, after imaging, cultures were subjected to kainate-induced Co^{2+} uptake labeling [$Co^{2+}(+)$ neurons], as previously described (23, 29).

After Co^{2+} loading (by exposure to 100 μM kainate with 2.5 mM Co^{2+}), intracellular Co^{2+} is precipitated by using $(NH_4)_2S$, fixed, and the stain silver enhanced by a modified Timm's stain procedure (14). After staining, dishes were reinserted in the microscope stage and fields rematched.

In the Fura-2FF Ca^{2+} imaging experiments, Ca-A/K(+) neurons were preidentified by applying a short (10 sec) pulse of 100 μM kainate in the presence of the nonselective VSCC blocker Gd^{3+} (10 μM; ref. 30) to elicit selective Ca^{2+} entry through Ca-A/K channels. In control experiments [three experiments, 39 $Co^{2+}(+)$ cells] over 90% of neurons loaded with Fura-2FF that showed an abrupt $[Ca^{2+}]_i$ rise on kainate/Gd^{3+} exposure were $Co^{2+}(+)$, and over 90% of $Co^{2+}(+)$ neurons present showed abrupt $[Ca^{2+}]_i$ rises.

RESULTS

Comparison of $\Delta[Zn^{2+}]_i$ On Activation of NMDA Channels, VSCC, and Ca-A/K Channels. The present study first set out to quantitatively compare $\Delta[Zn^{2+}]_i$ in cortical neurons occurring in response to Zn^{2+} influx through NMDA channels, VSCC, and Ca-A/K channels. Because NMDA channels and VSCC are expressed in virtually all neurons, the resultant $\Delta[Zn^{2+}]_i$ can be assessed in the overall neuronal population. In contrast, large numbers of Ca-A/K channels are expressed only in discrete subsets of central neurons [Ca-A/K(+) neurons] that can be identified either histochemically (by kainate-stimulated Co^{2+} uptake labeling; refs. 14, 23, 29, 31) or dynamically, as those exhibiting distinct kainate-triggered rises in $[Ca^{2+}]_i$ in the presence of VSCC antagonists. Control experiments (see *Materials and Methods*) have demonstrated that these approaches identify near identical sets of neurons that constitute a small minority (about 15%) of total neurons in cortical cultures (13, 15, 31).

Because high-affinity Zn^{2+} probes could underestimate high $[Zn^{2+}]_i$ ion levels associated with neurotoxicity, for present studies we chose to use the lower-affinity ($K_d \approx 1$ μM) Zn^{2+}-selective (Ca^{2+} and Mg^{2+} insensitive) indicator, Newport green (15, 18, 32). After loading cortical cultures with Newport green and recording baseline fluorescence, the cultures were exposed for 5 min to 300 μM Zn^{2+} in the presence of kainate (100 μM + 10 μM MK-801), high-K^+ (50 mM + 10 μM MK-801 and NBQX), or NMDA (100 μM + 10 μM NBQX), and fluorescence monitored for an additional 60 min. NMDA exposures caused a very slight $\Delta[Zn^{2+}]_i$ of <100 nM, near the lower limit of detection of the dye. The high-K^+ exposures caused substantially greater $\Delta[Zn^{2+}]_i$, with most neurons achieving levels in the 500- to 700-nM range. There were no significant differences in $\Delta[Zn^{2+}]_i$ between Ca-A/K(+) and Ca-A/K(−) neurons on either NMDA or high-K^+ exposure. In contrast, on kainate exposure, two distinct types of responses were seen. In most neurons, $\Delta[Zn^{2+}]_i$ were very similar to those observed on high-K^+ exposure. However, a minority of neurons showed much greater $\Delta[Zn^{2+}]_i$, with increases to several micromolar. Indicating preferential Zn^{2+} permeation through Ca-A/K channels, there was a near one-to-one correlation between neurons showing the greatest $\Delta[Zn^{2+}]_i$ in response to kainate and the Ca-A/K(+) neurons (Figs. 1 and 2; Table 1).

Zn^{2+} Entry Through Ca-A/K Channels Triggers ROS Generation and Mitochondrial Depolarization. Rapid Ca^{2+} influx through either NMDA channels or through Ca-A/K channels has been reported to trigger mitochondrial depolarization and ROS generation of mitochondrial origin (17, 19–22). In light of these precedents and of studies indicating that Zn^{2+} can interfere with mitochondrial function (33–35), we next explored the ability of agonist-triggered Zn^{2+} entry to induce ROS production. ROS generation was monitored by measuring changes in fluorescence of cells loaded with HEt, a dye that readily permeates living cells and is reported to be
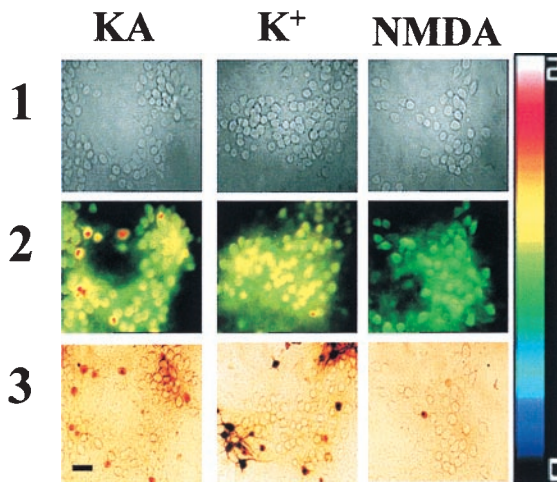
FIG. 1. Kainate + Zn^{2+} exposures trigger large Newport green fluorescence increases in Ca-A/K(+) neurons. Cortical cultures were loaded with Newport green and exposed for 5 min to 300 μM Zn^{2+} with 100 μM kainate (+10 μM MK-801; KA); with 50 mM K^+ (+10 μM MK-801, 10 μM NBQX; K^+); or with 100 μM NMDA (+10 μM NBQX; NMDA). In each experiment, baseline images were obtained under visible light before the exposure (*1*) and fluorescence images obtained before and at the end of the 5 min exposure. Because variability in dye loading causes differences in absolute fluorescence between neurons, Zn^{2+}-dependent signal increases are shown as pseudocolor ratios of peak/basal fluorescence (*2*). After the exposure, the Ca-A/K(+) neurons were identified by kainate stimulated Co^{2+} uptake (*3*). Note the relatively selective $[Zn^{2+}]_i$ increase in Ca-A/K(+) neurons after kainate exposure. (Bar = 50 μm.) The pseudocolor bar shows ratio excursions for row 2.

selectively oxidized by superoxide radicals into the highly fluorescent compound, ethidium (22, 36). In addition, the relative resistance of HEt to autooxidation and photooxidation (in comparison to other oxidation-sensitive fluorescent dyes; refs. 20, 21) allows prolonged periods of fluorescence monitoring needed for present studies.
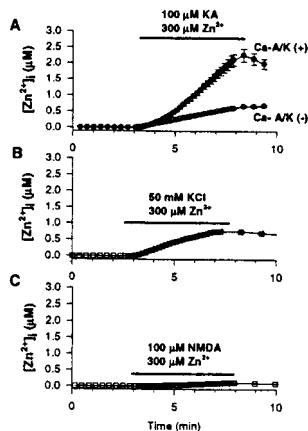

FIG. 2. Kainate + Zn^{2+} exposures trigger high $\Delta[Zn^{2+}]_i$ in Ca-A/K(+) neurons. Cortical cultures were loaded with Newport green and, after recording baseline fluorescence, were exposed for 5 min to 300 μM Zn^{2+} with 100 μM kainate (+10 μM MK-801; *A*); with 50 mM K^+ (+10 μM MK-801, 10 μM NBQX; *B*); or with 100 μM NMDA (+10 μM NBQX; *C*). Ca-A/K(+) neurons are shown only in *A*, as control experiments showed no difference in $\Delta[Zn^{2+}]_i$ between Ca-A/K(+) and Ca-A/K(−) neurons after high-K^+ or NMDA exposures. Traces show mean (±SEM) of 13 Ca-A/K(+) neurons (*A*) and ≥44 of either Ca-A/K(−) (*A*) or total neurons (*B*, *C*) from one experiment representative of ≥5. Note the particularly high kainate-triggered $\Delta[Zn^{2+}]_i$ in Ca-A/K(+) neurons and lower $\Delta[Zn^{2+}]_i$ in all neurons after high-K^+ or NMDA exposures.

Because Ca^{2+} entry can trigger ROS generation, to isolate pure Zn^{2+}-dependent effects, HEt-loaded cultures were switched into a Ca^{2+}-free buffer and baseline fluorescence monitored for 10 min. Zn^{2+} (300 μM) was then added in the presence of kainate (300 μM + 10 μM MK-801), high-K^+ (50 mM + 10 μM MK-801 and NBQX), or NMDA (300 μM + 10 μM NBQX) in Ca^{2+}-free buffer for 10 min. After washout into Ca^{2+}-free buffer containing 500 μM of the cell impermeant Zn^{2+} chelator, EDTA, MK-801, and NBQX, HEt fluorescence was monitored for an additional 20 min. HEt fluorescence changes paralleled the agonist-triggered $\Delta[Zn^{2+}]_i$. Whereas NMDA and high-K^+ exposures caused little fluorescence increase, kainate exposures caused marked increases only in the Ca-A/K(+) neuronal population (Fig. 3, 4). Indicating that this kainate-triggered ROS production was Zn^{2+} dependent, addition of the cell-permeant Zn^{2+} chelator N,N′,N′-tetrakis (2-pyridylmethyl)ethylenediamine before and after (but not during) the Zn^{2+}/kainate exposure abolished the fluorescence change (data not shown). Neurotoxicity experiments revealed a brief (5-min) exposure to kainate (50 μM) + Zn^{2+} (50 μM) to cause selective injury to Ca-A/K neurons [68 ± 4% Ca-A/K(+) neuronal damage vs. <20% overall neuronal loss]. Consistent with previous studies examining effects of antioxidants on chronic Zn^{2+} toxicity (37), addition of the 21-aminosteroid antioxidant U74500A (38) after the exposure decreased Ca-A/K(+) injury by >50% (to 32 ± 6%; n = seven to eight cultures from three platings each condition; P < .001 by Student's t test).

Mitochondria are a major source of ROS generation in response to rapid Ca^{2+} influx through NMDA channels (19–22) or Ca-A/K channels (17). To test the hypothesis that mitochondria are the primary source of the Zn^{2+}-dependent ROS generation, subsequent experiments examined effects of the complex I inhibitor rotenone (10 μM) on the kainate + Zn^{2+}-triggered HEt fluorescence changes in Ca-A/K(+) neurons. HEt-loaded cultures were preexposed to rotenone for 40 min before, during, and after addition of Zn^{2+} (300 μM) with kainate (300 μM), as above. To avoid effects due to endogenous glutamate release, MK-801 and NBQX (both at 10 μM) were included during the pre- and postexposure periods. Under these conditions HEt fluorescence increases in Ca-A/K(+) neurons were almost completely eliminated (normalized increase of 1.33 ± 0.07 in Ca-A/K(+) neurons in the absence of rotenone vs. 0.43 ± 0.04 with rotenone; n ≥ 39 neurons, four experiments each condition; P < 0.001 by Student's t test).

To further assess Zn^{2+} interaction with mitochondria, subsequent studies made use of the mitochondrial potential ($\Delta\psi$)-sensitive dye, TMRE. TMRE equilibrates rapidly between cellular compartments as a function of potential differences; the rapid loss of fluorescence from cellular domains rich in mitochondria is indicative of the loss of $\Delta\psi$ (27). Neurons were loaded with TMRE and after baseline recording were exposed to kainate (100 μM + 10 μM MK-801) + Zn^{2+} (100 μM) in Ca^{2+}-free buffer. On addition of kainate + Zn^{2+}, a rapid increase in fluorescence was seen in virtually all neurons, followed by a rapid loss of fluorescence in the Ca-A/K(+) neurons (Fig. 5A), reflecting redistribution of dye from depolarized mitochondria (27, 39). The lack of comparable fluorescence change in Ca-A/K(−) neurons provides an internal control, indicating that the signal is caused by loss of $\Delta\psi$, as kainate induces Na^+-dependent neuronal depolarization in virtually all neurons. Kainate exposures without Zn^{2+} also caused no decrease in TMRE signal (data not shown).

A recent report by Budd *et al.* (40) suggested that loss of $\Delta\psi$ *per se* might cause voltage-dependent release of oxidized ethidium from mitochondria, possibly contributing to the HEt signal. Two sets of control experiments were carried out to address this issue. First, studies were carried out by using only 1 μM HEt, a concentration at which Budd *et al.* found ethidium to remain bound within mitochondria despite loss of $\Delta\psi$.

Table 1.   Summary of agonist-induced $\Delta[Zn^{2+}]_i$ and $\Delta[Ca^{2+}]_i$

[Ion]$_i$ (μM)	NMDA + Zn^{2+}, 5 experiments, 162 neurons	KCl + Zn^{2+}, 6 experiments, 223 neurons	Kainate + Zn^{2+}, 7 experiments		Kainate + Ca^{2+}, 5 experiments	
			Ca-A/K(+), 31 neurons	Ca-A/K(−), 345 neurons	Ca-A/K(+), 33 neurons	Ca-A/K(−), 217 neurons
Peak at 5 min	0.04 + 0.003*	0.58 ± 0.02	2.3 ± 0.02	0.64 ± 0.03	34.0 ± 3.0	7.8 ± 0.2
Recovery at 60 min	<0.01*	0.12 ± 0.01	0.54 ± 0.05	0.21 ± 0.01	<1.5*#	<1.5*#

For $\Delta[Zn^{2+}]_i$ measurements, cortical cultures were loaded with Newport green and exposed for 5 min to 300 μM Zn^{2+} with 100 μM kainate (+10 μM MK-801); with 50 mM K$^+$ (+10 μM MK-801, 10 μM NBQX); or with 100 μM NMDA (+10 μM NBQX), as in Fig. 2. For $\Delta[Ca^{2+}]_i$ measurements, cultures were loaded with Fura-2FF and exposed for 5 min to 100 μM kainate in the presence of 1.8 mM Ca^{2+} (+10 μM MK-801), as in Fig. 6. Values in table show mean (±SEM) peak levels (at end of 5-min exposure) and levels 60 min after washout of the agonist, compiled from ≥ experiments. *Indicates that calibrated values are below the threshold for accurate quantification with the indicator. # indicates the complete recovery of [Ca^{2+}]$_i$ to basal levels (<150 nM) within 60 min after the exposures in control experiments using the high-affinity indicator fura-2.

Under these conditions, despite low signal intensity causing substantial loss of resolution, kainate + Zn^{2+} still triggered selective increases in HEt fluorescence in Ca-A/K(+) neurons (normalized increase of 1.04 ± 0.10 in Ca-A/K(+) neurons vs. 0.59 ± 0.01 in Ca-A/K(−) neurons, n ≥ 17 cells from six experiments). Secondly, in light of above observations that rotenone blocked HEt oxidation, we examined the effect of rotenone on Zn^{2+}-dependent loss of $\Delta\psi$. Indeed, addition of rotenone (10 μM) for 30 min before and during exposure to kainate (100 μM + 10 μM MK-801) + Zn^{2+} (100 μM) resulted in greater loss of $\Delta\psi$ in both Ca-A/K(+) and Ca-A/K(−) neurons than was observed in the absence of rotenone (Fig. 5B). Thus, the Zn^{2+}-dependent HEt signal that is blocked by rotenone cannot be simply caused by loss of $\Delta\psi$ and most likely reflects ROS production.

The High Toxic Potency of Zn^{2+} May Reflect the Protracted Time Course of $\Delta[Zn^{2+}]_i$ and Associated ROS Generation. Toxicity experiments have suggested that Zn^{2+} entry acts more

potently than Ca^{2+} entry to trigger neurodegeneration. Indeed, a brief (5- to 10-min) exposure to kainate in the presence of only 100 μM Zn^{2+} suffices to trigger degeneration of >80% of the $Co^{2+}(+)$ neuronal population (13, 14), whereas much less (<50%) injury to these neurons results from identical exposures when physiologic (1.8 mM) Ca^{2+} is substituted for the Zn^{2+} (31). Initial attempts to understand this difference in potency examined the Ca^{2+} or Zn^{2+} concentration dependence of kainate-triggered HEt fluorescence changes in Ca-A/K(+) neurons. Surprisingly, while exposures in the presence of 100–300 μM Zn^{2+} caused large and consistent increases in HEt fluorescence, fluorescence increases were also seen in many Ca-A/K(+) neurons after exposures in the presence of these same levels of Ca^{2+} (data not shown).

Alternatively, the greater toxicity of Zn^{2+} could be explained on a temporal basis, with the neurons recovering from Ca^{2+}-dependent effects more rapidly than from Zn^{2+}-dependent effects. In cultures loaded with the low-affinity Ca^{2+}-sensitive dye Fura-2FF ($K_d \approx 35 \mu$M; ref. 26), a 5-min kainate exposure (100 μM) in 1.8 mM Ca^{2+} triggered a rapid [Ca^{2+}]$_i$ rise in Ca-A/K(+) neurons to peak levels near 30 μM [Δ[Ca^{2+}]$_i$ in Ca-A/K(−) neurons was much less; Fig. 6 A and B]. In virtually every case, [Ca^{2+}]$_i$ in Ca-A/K(+) neurons
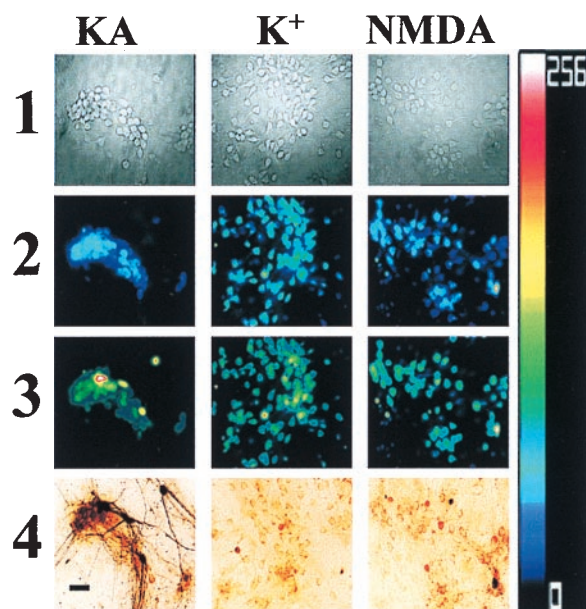

FIG. 3.   Kainate + Zn^{2+} exposures trigger selective ROS generation in Ca-A/K(+) neurons. Cortical cultures were loaded with HEt and exposed for 10 min in Ca^{2+}-free buffer to 300 μM Zn^{2+} with 300 μM kainate (+10 μM MK-801; KA); with 50 mM K$^+$ (+10 μM MK-801, 10 μM NBQX; K$^+$); or with 300 μM NMDA (+10 μM NBQX; NMDA). In each experiment, baseline images were obtained under visible light before the exposure (*1*) and fluorescence images obtained before (*2*) and 20 min after the end of the 10-min exposure (*3*). After the exposure, the Ca-A/K(+) neurons were identified by kainate-stimulated Co^{2+} uptake (*4*). Note the relatively selective increases in HEt fluorescence in Ca-A/K(+) neurons after kainate exposure. (Bar = 50 μm.) The pseudocolor bar shows the 8-bit fluorescence intensity scale (rows *2, 3*).
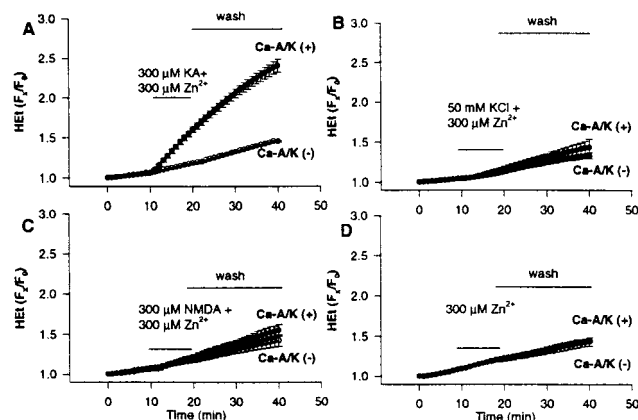

FIG. 4.   Time course of agonist-triggered ROS generation. Cortical cultures were loaded with HEt, switched into Ca^{2+}-free buffer, and, after recording baseline fluorescence, were exposed for 10 min to 300 μM Zn^{2+} with 300 μM kainate (+10 μM MK-801; *A*); with 50 mM K$^+$ (+10 μM MK-801, 10 μM NBQX; *B*); with 300 μM NMDA (+10 μM NBQX; *C*); or with buffer alone (+10 μM MK-801, 10 μM NBQX; *D*). Cultures were then washed into Ca^{2+}-free buffer containing 500 μM EDTA, 10 μM MK-801, and 10 μM NBQX. HEt fluorescence changes for each neuron are expressed as the ratio of fluorescence at each time point (F$_x$) to its own baseline fluorescence (F$_0$). Traces show mean (±SEM) of 86 Ca-A/K(+) and >800 Ca-A/K(−) neurons from 12 experiments (*A*) or ≥20 Ca-A/K(+) and ≥140 Ca-A/K(−) neurons from 4–5 experiments (*B–D*). Note the marked increase in HEt fluorescence only in the case of kainate exposures to Ca-A/K(+) neurons.
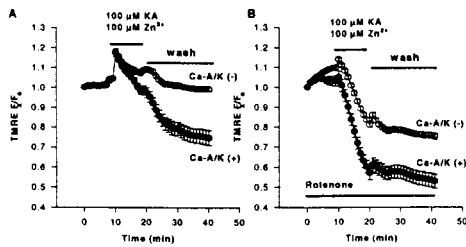
FIG. 5. Kainate + Zn^{2+} exposure triggers selective mitochondrial depolarization (loss of $\Delta\psi$) in Ca-A/K(+) neurons. Cultures were loaded with TMRE, switched into Ca^{2+}-free buffer, and, after recording baseline fluorescence, were exposed for 10 min to 100 μM Zn^{2+} with 100 μM kainate (+10 μM MK-801; *A*), or were identically exposed but with the addition of rotenone (10 μM) 30 min before, during, and after the exposure (*B*). Cultures were then washed into Ca^{2+}-free buffer containing 500 μM EDTA, 10 μM MK-801, and 10 μM NBQX. Fluorescence changes for each neuron are expressed as the ratio of fluorescence at each time point (F_x) to its own baseline fluorescence. Traces show the means ±SEM of TMRE fluorescence in mitochondrial-rich regions of ≥28 Ca-A/K(+) and ≥175 Ca-A/K(−) neurons from seven experiments each. Note the selective loss of TMRE fluorescence, indicative of loss of $\Delta\psi$, in Ca-A/K(+) neurons (*A*) and enhanced loss of $\Delta\psi$ in both Ca-A/K(+) and Ca-A/K(−) neurons in the presence of rotenone (*B*).

recovered to basal levels within 45 min. In contrast, in Newport green-loaded cultures, identical exposure to kainate with 300 μM Zn^{2+} resulted in peak $[Zn^{2+}]_i$ levels in Ca-A/K(+)

FIG. 6. Comparative time course of $\Delta[Cation]_i$ and ROS generation after pulse kainate exposure in the presence of Zn^{2+} or Ca^{2+}: greater persistence of Zn^{2+}-dependent effects. (*A* and *B*) Time course of $\Delta[Cation]_i$. Cortical cultures were loaded with either Fura-2FF (*A*) or Newport green (*B*), and, after recording baseline fluorescence, were exposed for 5 min to 100 μM kainate in the presence of 1.8 mM Ca^{2+} (+10 μM MK-801; *A*) or were identically exposed except for the addition of 300 μM Zn^{2+} (*B*). Cultures were then washed and monitored for an additional 60 min. Traces show mean calibrated values (±SEM) of ≥7 Ca-A/K(+) neurons, 50 Ca-A/K(-) neurons from one experiment representative of ≥5. Note the slow recovery of $\Delta[Zn^{2+}]_i$ compared with that of $\Delta[Ca^{2+}]_i$ in Ca-A/K(+) neurons. (*C* and *D*) Time course of ROS generation. Cortical cultures were loaded with HEt and, after baseline recording in Ca^{2+}-free buffer, were exposed for 5 min to 100 μM kainate in the presence of 1.8 mM Ca^{2+} (+10 μM MK-801; *C*) or were identically exposed except for substitution of 300 μM Zn^{2+} for Ca^{2+} (*D*). Cultures were then washed into Ca^{2+}-free buffer (+500 μM EDTA, 10 μM MK-801, 10 μM NBQX) and monitored for 60 more min. HEt fluorescence changes for each neuron are expressed as the ratio of fluorescence at each time point (F_x) to its own baseline fluorescence (F_0). Traces show mean values (±SEM) of ≥7 Ca-A/K(+), 50 Ca-A/K(-) neurons from a single experiment representative of four. Note the prolonged increase in HEt fluorescence in Ca-A/K(+) neurons only in the case of kainate + Zn^{2+} exposures.

neurons of 2–3 μM, with only partial recovery 60 min after the exposure (Fig. 6; Table 1).

Subsequent experiments compared the time course of ROS generation in Ca-A/K(+) neurons after pulse (5 min) kainate exposures in the presence of Ca^{2+} or Zn^{2+}. HEt-loaded cultures were exposed for 5 min to kainate (100 μM) either with 1.8 mM Ca^{2+} or with 300 μM Zn^{2+}, followed by washout (into Ca^{2+}-free media containing 1 mM EDTA, MK-801, and NBQX) and monitoring for 60 more minutes. The kainate + Ca^{2+} exposures caused a rapid increase in HEt fluorescence in Ca-A/K(+) neurons, reaching a plateau (suggesting a cessation of ROS production) shortly after washout, which generally persisted for the duration of the recording. In contrast, while the initial increase in HEt fluorescence in Ca-A/K(+) neurons was more gradual during the kainate + Zn^{2+} exposures, the fluorescence increased steadily over 60 min after the washout (Fig. 6 *C* and *D*).

DISCUSSION

The motivation for the present study resulted from observations that presynaptic vesicular Zn^{2+} can be released from excitatory terminals and can translocate into postsynaptic neurons, where it may well contribute to the selective neurodegeneration that occurs in conditions such as global ischemia or epilepsy (5–8). The study thus first set out to characterize $\Delta[Zn^{2+}]_i$ resulting from prolonged "toxic" activation of three potential routes of influx, NMDA channels, VSCC, and Ca-A/K channels. To achieve comparable prolonged activation of each of these channels, the relatively nondesensitizing agonist, kainate, was chosen over AMPA to activate AMPA/kainate channels. Thus, by using the low-affinity Zn^{2+} selective indicator, Newport green, present studies provide clear distinction between $\Delta[Zn^{2+}]_i$ on activation of each of the three routes and quantitatively confirm the rank order of permeation suggested by toxicity studies (Ca-A/K channels > VSCC > NMDA channels), with influx through Ca-A/K channels providing by far the greatest $\Delta[Zn^{2+}]_i$. Indeed, the ratio of peak $[Zn^{2+}]_i$ levels in the Ca-A/K(+) neurons to extracellular levels ($\approx$3 μM/300 μM) is not much less than the ratio for Ca^{2+} ($\approx$30 μM/1,800 μM), suggesting that the permeability of Ca-A/K channels to Zn^{2+} might be comparable to their permeability for Ca^{2+}. Furthermore, as Ca-A/K channels, unlike VSCC, are likely concentrated in postsynaptic regions of dendrites adjacent to sites of presynaptic release, we propose the hypothesis that Ca-A/K channels constitute the principal physiologic route of Zn^{2+} translocation.

Whereas Zn^{2+} is a potent regulator of many intracellular enzymes (41–43), several previous studies provide precedent for the hypothesis that metabolic/oxidative effect might be of particular importance to Zn^{2+}-mediated injury. First, like Ca^{2+}, Zn^{2+} can be taken up by the mitochondrial uniporter (44), providing a route for entry into mitochondria, where it can interfere with mitochondrial function and injure neurons (33–35). Present data, in addition to demonstrating an ability of intracellular Zn^{2+} to directly interact with mitochondria and cause ROS production, provide information about levels of $[Zn^{2+}]_i$ needed for the ROS generation. Specifically, sharp increases in the rate of HEt oxidation were seen only in the case of micromolar $[Zn^{2+}]_i$ occurring after entry through Ca-A/K channels, whereas the several hundred nanomolar levels achieved on influx through VSCC caused no comparable fluorescence change. This apparent high degree of selectivity could reflect a threshold $\Delta[Zn^{2+}]_i$ necessary for mediating its toxic effect (for instance, the mitochondrial uniporter may carry Zn^{2+} with a K_d of $\approx$1 μM; ref. 44) or could reflect source specificity (45). For instance, Zn^{2+} entering through Ca-A/K channels may often be more spatially constrained than that entering through VSCC, causing higher local $\Delta[Zn^{2+}]_i$. It is also possible that the apparent threshold reflects the sensitivity
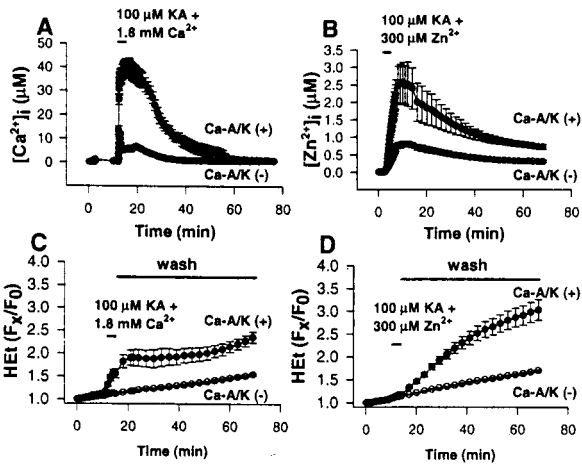
of the present assay, such that lower levels of ROS production occurring on Zn^{2+} entry through VSCC are not detected. In any case, present studies indicating antioxidant protection against selective injury resulting from rapid kainate-stimulated Zn^{2+} influx, like previous studies showing antioxidant efficacy on chronic Zn^{2+} toxicity (37), lend support to the idea that the Zn^{2+}-dependent mitochondrial ROS generation contributes directly to consequent neurodegeneration.

Our findings may also provide insight into the high neurotoxic potency of Zn^{2+}. Present data lend support to the idea that the high toxic potency of Zn^{2+} compared with Ca^{2+} may largely reflect a much greater persistence of its effects. Indeed, very high $[Ca^{2+}]_i$ levels recovered completely within 45 min, reflecting the effectiveness of the Ca^{2+} homeostatic mechanisms. Such an ability to recover and maintain $[Ca^{2+}]_i$ levels, even after lethal excitotoxic insults, is evidenced further by observations that $[Ca^{2+}]_i$ levels normalize after brief intense glutamate exposures, until a markedly delayed $[Ca^{2+}]_i$ rise signals imminent death (46, 47). In contrast, the relative lack of recovery of considerably lower $[Zn^{2+}]_i$ levels in Ca-A/K neurons correlates well with the markedly greater persistence of ROS generation after a brief kainate $+ Zn^{2+}$ exposure, suggesting that a relative paucity of clearance capacity may substantially underlie its high toxic potency.

Both glutamate-mediated excitotoxicity and oxidative stress have been implicated in acute neuronal injury as occurs in global ischemia, epilepsy, or trauma (48). Whereas previous studies demonstrating rapid Ca^{2+} influx through NMDA channels and consequent ROS production would predict a predominant role of NMDA receptors in those conditions, animal studies have suggested a surprisingly large contribution of AMPA/kainate receptors (49, 50). Present results may bear on this issue by suggesting the possibility that the large contribution of AMPA/kainate receptors could in part reflect selective Zn^{2+} permeation through Ca-A/K(+) channels and consequent persistent mitochondrial impairment and ROS generation.

1. Dansher, G. (1984) in *The Neurobiology of Zinc*, eds. Frederickson, C. J., Howell, G. A. & Kasarkis, E. J. (Liss, New York), pp. 273–287.
2. Perez-Clausell, J. & Danscher, G. (1985) *Brain. Res.* **337,** 91–98.
3. Assaf, S. Y. & Chung, S. H. (1984) *Nature (London)* **308,** 734–736.
4. Howell, G. A., Welch, M. G. & Frederickson, C. J. (1984) *Nature (London)* **308,** 736–738.
5. Sloviter, R. S. (1985) *Brain Res.* **330,** 150–153.
6. Frederickson, C. J., Hernandez, M. D. & McGinty, J. F. (1989) *Brain Res.* **480,** 317–321.
7. Tonder, N., Johansen, F. F., Frederickson, C. J., Zimmer, J. & Diemer, N. H. (1990) *Neurosci. Lett.* **109,** 247–252.
8. Koh, J. Y., Suh, S. W., Gwag, B. J., He, Y. Y., Hsu, C. Y. & Choi, D. W. (1996) *Science* **272,** 1013–1016.
9. Suh, S. W., Koh, J. Y. & Choi, D. W. (1996) *Soc. Neurosci. Abs.* **26,** 823.6.
10. Weiss, J. H., Hartley, D. M., Koh, J. Y. & Choi, D. W. (1993) *Neuron* **10,** 43–49.
11. Freund, W. D. & Reddig, S. (1994) *Brain Res.* **654,** 257–264.
12. Koh, J. Y. & Choi, D. W. (1994) *Neuroscience* **60,** 1049–1057.
13. Yin, H. Z. & Weiss, J. H. (1995) *NeuroReport* **6,** 2553–2556.
14. Yin, H. Z., Ha, D., Carriedo, S. G. & Weiss, J. H. (1998) *Brain Res.* **781,** 45–56.
15. Sensi, S. L., Canzoniero, L. M., Yu, S. P., Ying, H. S., Koh, J. Y., Kerchner, G. A. & Choi, D. W. (1997) *J. Neurosci.* **17,** 9554–9564.
16. Hyrc, K., Handran, S. D., Rothman, S. M. & Goldberg, M. P. (1997) *J. Neurosci.* **17,** 6669–6677.
17. Carriedo, S. G., Yin, H. Z., Sensi, S. L. & Weiss, J. H. (1998) *J. Neurosci.* **18,** 7727–7738.
18. Haugland, R. P. (1996) *Handbook of Fluorescent Probes and Research Chemicals*, ed. Spencer, M. T. Z. (Molecular Probes, Eugene, OR), 6th Ed., pp. 530–540.
19. Lafon-Cazal, M., Pietri, S., Culcasi, M. & Bockaert, J. (1993) *Nature (London)* **364,** 535–537.
20. Reynolds, I. J. & Hastings, T. G. (1995) *J. Neurosci.* **15,** 3318–3327.
21. Dugan, L. L., Sensi, S. L., Canzoniero, L. M., Handran, S. D., Rothman, S. M., Lin, T. S., Goldberg, M. P. & Choi, D. W. (1995) *J. Neurosci.* **15,** 6377–6388.
22. Bindokas, V. P., Jordan, J., Lee, C. C. & Miller, R. J. (1996) *J. Neurosci.* **16,** 1324–1336.
23. Yin, H., Turetsky, D., Choi, D. W. & Weiss, J. H. (1994) *Neurobiol. Dis.* **1,** 43–49.
24. Grynkiewicz, G., Poenie, M. & Tsien, R. Y. (1985) *J. Biol. Chem.* **260,** 3440–3450.
25. Arslan, P., Di Virgilio, F., Beltrame, M., Tsien, R. Y. & Pozzan, T. (1985) *J. Biol. Chem.* **260,** 2719–2727.
26. Golovina, V. A. & Blaustein, M. P. (1997) *Science* **275,** 1643–1648.
27. Farkas, D. L., Wei, M., Febbroriello, P., Carson, J. H. & Loew, L. M. (1989) *Biophys. J.* **56,** 1053–1068.
28. Koh, J. & Choi, D. W. (1987) *J. Neurosci. Methods* **20,** 83–90.
29. Pruss, R. M., Akeson, R. L., Racke, M. M. & Wilburn, J. L. (1991) *Neuron* **7,** 509–519.
30. Yu, S. P., Yeh, C. H., Sensi, S. L, Gwag, B. J., Canzoniero, L. M., Farhangrazi, Z. S., Ying, H. S., Tian, M., Dugan, L. L. & Choi, D. W. (1997) *Science* **278,** 114–117.
31. Turetsky, D. M., Canzoniero, L. M., Sensi, S. L., Weiss, J. H., Goldberg, M. P. & Choi, D. W. (1994) *Neurobiol. Dis.* **1,** 101–110.
32. Canzoniero, L. M., Sensi, S. L. & Choi D. W. (1997) *Neurobiol. Dis.* (**3–4**), 275–279.
33. Skulachev, V. P., Chistyakov, V. V., Jasaitis, A. A. & Smirnova, E. G. (1967) *Biochem. Biophys. Res. Commun.* **26,** 1–6.
34. Nicholls, P. & Malviya, A. N. (1968) *Biochemistry* **7,** 305–310.
35. Manev, H., Kharlamov, E., Uz, T., Mason, R. P. & Cagnoli, C. M. (1997) *Exp. Neurol.* **146,** 171–178.
36. Satoh, T., Numakawa, T., Abiru, Y., Yamagata, T., Ishikawa, Y., Enokido, Y. & Hatanaka, H. (1998) *J. Neurochem.* **70,** 316–324.
37. Kim, E. Y., Koh, J. Y., Kim, Y. H., Sohn, S. H. & Gwag, B. J. (1997) *Soc. Neurosci. Abs.* **27,** 252.12.
38. Monyer, H., Hartley, D. M. & Choi, D. W. (1990) *Neuron* **5,** 121–126.
39. Schinder, A. F., Olson, E. C., Spitzer, N. C. & Montal, M. (1996) *J. Neurosci.* **16,** 6125–6133.
40. Budd, S. L., Castilho, R. F. & Nicholls, D. G. (1997) *FEBS Lett.* **415,** 21–24.
41. Vallee, B. L. & Falchuk, K. H. (1993) *Physiol. Rev.* **1,** 79–118.
42. Berg, J. M. & Shi, Y. (1996) *Science* **271,** 1081–1085.
43. Frederickson, C. J. (1989) *Int. Rev. Neurobiol.* **31,** 145–238.
44. Saris, N. E. & Niva K. (1994) *FEBS Lett.* **356,** 195–198.
45. Tymianski, M., Charlton, M. P., Carlen, P. L. & Tator, C. H. (1993) *J. Neurosci.* **13,** 2085–2104.
46. Randall, R. D. & Thayer, S. A. (1992) *J. Neurosci.* **12,** 1882–1895.
47. Dubinsky, J. M. (1993) *J. Neurosci.* **13,** 623–631.
48. Choi, D. W. (1988) *Neuron* **1,** 623–634.
49. Sheardown, M. J., Nielsen, E. O., Hansen, A. J., Jacobsen, P. & Honore, T. (1990) *Science* **247,** 571–574.
50. Wrathall, J. R., Choiniere, D. & Teng, Y. D. (1994) *J. Neurosci.* **14,** 6598–6607.